On the Origin of the Temperature Dependence of the Supercoiling Free Energy

Jeffrey J. Delrow, Patrick J. Heath, and J. Michael Schurr
Department of Chemistry, University of Washington, Seattle, Washington 98195-1700 USA

ABSTRACT Monte Carlo simulations using temperature-invariant torsional and bending rigidities fail to predict the rather steep decline of the experimental supercoiling free energy with increasing temperature, and consequently fail to predict the correct sign and magnitude of the supercoiling entropy. To illustrate this problem, values of the twist energy parameter (E_T), which governs the supercoiling free energy, were simulated using temperature-invariant torsion and bending potentials and compared to experimental data on pBR322 over a range of temperatures. The slope, $-dE_T/dT$, of the simulated values is also compared to the slope derived from previous calorimetric data. The possibility that the discrepancies arise from some hitherto undetected temperature dependence of the torsional rigidity was investigated. The torsion elastic constant of an 1876-bp restriction fragment of pBR322 was measured by time-resolved fluorescence polarization anisotropy of intercalated ethidium over the range 278–323 K, and found to decline substantially over that interval. Simulations of a 4349-bp model DNA were performed using these measured temperature-dependent torsional rigidities. The slope, $-dE_T/dT$, of the simulated data agrees satisfactorily with the slope derived from previous calorimetric measurements, but still lies substantially below that of Duguet's data. Models that involve an equilibrium between different secondary structure states with different intrinsic twists and torsion constants provide the most likely explanation for the variation of the torsion constant with T and other pertinent observations.

INTRODUCTION

The deformational free energy of supercoiled DNAs has been shown to facilitate various biochemical processes, including transcription, replication, recombination, and the binding of unwinding proteins, all of which involve either the unwinding of DNA or the close juxtaposition of proteins bound to different sites on the same DNA (Gellert, 1981; Wang, 1985; Bauer and Gallo, 1989; Rippe et al., 1995; Langowski et al., 1985; Clendenning and Schurr, 1994a). There is also considerable evidence that under some conditions superhelical strain can promote long-range or extensive transitions in duplex secondary structure (Shibata et al., 1984; Wu et al., 1988, 1991; Wu and Schurr, 1989; Song et al., 1990; Naimushin et al., 1994). Such a transition may enable long-range signaling via a structural transmission effect between an enhancer protein bound at one site and an RNA polymerase complex bound ~80 bp away (Parekh and Hatfield, 1996). Knowledge of the supercoiling free energies and tertiary structures of superhelical DNAs alone might suffice to understand the role of supercoiling in some of these processes. However, understanding the connection between supercoiling on one hand and transitions in secondary structure on the other is likely to involve the separate entropy and enthalpy of supercoiling, as detailed subsequently. In any case, the entropy and enthalpy of supercoiling constitute an important contemporary puzzle that merits investigation. Understanding the origin of the temperature dependence of the supercoiling free energy, which determines the separate enthalpy and entropy of supercoiling, is the primary objective of the present work.

The extent of deformation of a supercoiled DNA depends on its linking difference, $\Delta l = l - l_0$, where l is its linking number and l_0 its intrinsic twist. The variation of the supercoiling free energy (ΔG_{sc}) with linking difference has been investigated by both experiments and simulations.

Experiments on large (>2000 bp) supercoiled DNAs in the "normal" range of ionic strengths (i.e., 30–200 mM) indicate that the supercoiling free energy (ΔG_{sc}) varies nearly quadratically with Δl, not only at low levels of supercoiling (Pulleyblank et al., 1975; Depew and Wang, 1975; Shore and Baldwin, 1983; Horowitz and Wang, 1984; Naimushin et al., 1994), but also up to native superhelix density ($\sigma = -0.05$) in the case of p30δ DNA (Clendenning et al., 1994). That is,

$$\frac{\Delta G_{sc}}{RT} = E_T \frac{\Delta l^2}{N} \tag{1}$$

where N is the number of base pairs, R is the gas constant, T is the absolute temperature, and E_T is the twist energy parameter, which is independent of N for sufficiently large DNAs.

The predictions of Monte Carlo simulations depend on the value adopted for the torsional rigidity (C) (Gebe et al., 1995). The torsional rigidity is related to the torsion elastic constant between base pairs (α) by $C = h\alpha$, where $h = 3.4$ Å is the rise per base pair. Measurements of the time-resolved fluorescence polarization anisotropy (FPA) of intercalated ethidium yield values near $C = 2.0 \times 10^{-19}$ dyne cm^2 ($\alpha = 5.9 \times 10^{-12}$ dyne cm) for large linear and

Received for publication 5 March 1997 and in final form 31 July 1997.

Address reprint requests to Dr. J. Michael Schurr, Department of Chemistry, Campus Box 351700, University of Washington, Seattle, WA 98195-1700. Tel.: 206-543-6681; Fax: 206-685-8665; E-mail: schurr@chem.washington.edu.

0006-3495/97/11/2688/14 $2.00

circular plasmid DNAs, including p30δ (4752 bp) (Schurr et al., 1992; Heath et al., 1996). The same value of C is obtained by cyclization kinetics measurements on DNAs containing 340–350 bp (Taylor and Hagerman, 1990). When this value is employed in simulations of p30δ, the predicted supercoiling free energies follow Eq. 1 rather closely, in the sense that E_T is nearly constant over the range of Δl from 0 to native (−23 turns). Moreover, the predicted E_T values ($E_T \cong 1000$), light-scattering structure factors, and translational diffusion coefficients agree well with the corresponding experimental data for particular samples of p30δ at different superhelix densities (Gebe et al., 1995, 1996). A considerably larger torsional rigidity, $C = 3.0 \times 10^{-19}$ dyne cm^2, was obtained from measured topoisomer ratios of small circles containing 205–217 bp (Horowitz and Wang, 1984; Shimada and Yamakawa, 1985; Frank-Kamenetskii et al., 1985), and a still larger value, $C \cong 4.1 \times 10^{-19}$ dyne cm^2, was obtained by analyzing topoisomer ratios of 247-bp DNAs that were circularized in the presence of various concentrations of ethidium (Shore and Baldwin, 1983; Clendenning and Schurr, 1994b). However, these higher C values were recently shown to be induced by the coherent bending strain that prevails in such small circles and affects other properties that are sensitive to the "average" secondary structure (Heath et al., 1996). Such large values of the torsional rigidity are not applicable to either linear or larger ($N \geq 340$ bp) circular DNAs, which experience smaller coherent bending strains (Heath et al., 1996). Use of the higher value, $C = 3.0 \times 10^{-19}$ dyne cm^2, in the simulations yields a weaker than quadratic dependence of ΔG_{sc} on Δl, because E_T declines significantly with increasing magnitude of Δl (Klenin et al., 1991; Vologodskii and Cozzarelli, 1994; Gebe et al., 1995) and gives poor agreement between predicted and experimental ΔG_{sc} values for p30δ DNA at all Δl from 0 to native (Gebe et al., 1995).

Although simulations using the (constant) torsional rigidity ($C = 2.0 \times 10^{-19}$ dyne cm^2) predict ΔG_{sc} values and other properties in good agreement with experiments at ambient temperature, the predicted variation of E_T (or ΔG_{sc}) with temperature deviates rather far from the reported experimental observations. In particular, the experimental slopes, $-dE_T/dT$, exceed in magnitude the predicted values by severalfold. The relevant thermodynamic relations are

$$\Delta H_{sc} = \frac{\partial(\Delta G_{sc}/T)}{\partial(1/T)} = -T\frac{dE_T}{dT}RT\frac{\Delta l^2}{N} \qquad (2)$$

$$\Delta S_{sc} = \frac{\partial \Delta G_{sc}}{\partial T} = -\left(E_T + T\frac{dE_T}{dT}\right)R\frac{\Delta l^2}{N} \qquad (3)$$

If $-dE_T/dT$ were smaller than E_T/T, as previous simulations predict, then ΔS_{sc} would be negative and ΔH_{sc} would be smaller than ΔG_{sc}. However, in the event that $-dE_T/dT$ exceeds E_T/T, as is found experimentally, then ΔS_{sc} is positive and ΔH_{sc} exceeds ΔG_{sc}.

Simulations performed using T-independent values of the bending and twisting rigidities and of the effective hard-cylinder diameter invariably yield a small negative ΔS_{sc} (Vologodskii and Cozzarelli, 1994). This implies that the major contribution to ΔG_{sc} comes from a large positive ΔH_{sc}, which, however, does not exceed ΔG_{sc}. It also implies via Eq. 3 that $(-dE_T/dT)$ is less than E_T/T. This picture is conceptually reasonable, because the deformation of "springs" with T-independent torque constants is a purely endothermic process (large positive ΔH_{sc}), and the effect of supercoiling is to reduce the number of configurational states available to the DNA (small negative ΔS_{sc}). Nevertheless, the experiments present a rather different picture.

Seidl and Hinz (1984) performed microcalorimetric measurements on ColE1 *amp* plasmid DNAs (11,000 bp). Their data for the enthalpy of supercoiling at 310 K can be represented approximately by $\Delta H_{sc} = -2666RT(\Delta l^2/N)$ J/mol DNA. When combined with the relation $\Delta G_{sc} = \Delta H_{sc} - T\Delta S_{sc}$ and Eq. 1, using $E_T = 1000$ (Depew and Wang, 1975; Clendenning et al., 1994), this implies that $\Delta S_{sc} = 1666R(\Delta l^2/N)$, which is large and positive. In this case, ΔH_{sc} substantially exceeds ΔG_{sc}. When the experimental result for ΔH_{sc} is inserted into Eq. 2, one obtains $dE_T/dT = -8.6$ K^{-1}, so the experimental $(-dE_T/dT)$ substantially exceeds $E_T/T = 1000/310 = 3.23$ K^{-1} in this instance.

Duguet (1993) electrophoretically resolved topoisomer distributions that were created by relaxing pBR322 DNA (4363 bp) at various temperatures with topoisomerase I from a thermophile. By analyzing those distributions it was determined that $E_T = 1320$ for pBR322 at 308 K and that $dE_T/dT = -15.6 \pm 1$ K^{-1} over the range from 308 to 358 K. In this case, the experimental slope $(-dE_T/dT)$ is even larger than that noted above, which implies still larger positive values of ΔS_{sc} and ΔH_{sc}. It is also notable that Duguet's value, $E_T = 1320$ at 308 K, considerably exceeds the values measured for that same plasmid at 310 K by Horowitz and Wang (1984) and Naimushin et al. (1994), namely $E_T = 1130$ and 1155, respectively. However, the value reported for pBR322 at 293 K by Shore and Baldwin (1983), $E_T = 1610$, extrapolates to $E_T = 1340$ at 310 K with Duguet's slope. Thus in the case of pBR322, the E_T measurements of Shore and Baldwin (1983) and Duguet (1993) are ~17% larger than those of Horowitz and Wang (1984) and Naimushin et al. (1994). This "reproducible" discrepancy might be ascribed to long-lived metastable secondary structures in certain of these pBR322 samples. A similar "reproducible" discrepancy is found in the measured torsional rigidities of small ($N \leq 250$ bp) circular DNAs at 293 K, which appear to fall into either of two ranges, namely $C = (3.1–3.3) \times 10^{-19}$ or $(4.0–4.2) \times 10^{-19}$ dyne cm^2, regardless of the measurement method (Heath et al., 1996). Some evidence suggests that the latter higher value might prevail at equilibrium in such small circles, where the secondary structure is significantly altered by the bending strain (Heath et al., 1996). A variety of evidence for irreproducible behavior and long-lived metastable secondary structure(s) in pBR322 was presented and discussed previously (Wu et al., 1991; Naimushin et al., 1994). Such large

values of E_T as those reported by Shore and Baldwin (1983) and Duguet (1993) cannot be simulated by using the canonical value of the persistence length, $p = 500$ Å, and any previously (or currently) reported values of C. Only by using a larger value of P, or by using a C value that significantly exceeds the largest currently known experimental estimate could quantitative agreement between the predicted ΔG_{sc} and E_T values and those reported by Duguet be achieved.

Naimushin et al. (1994) reported E_T values for pBR322 at 293 and 310 K. Although the error in the estimated slope, $dE_T/dT = -11 \pm 8\ K^{-1}$, is comparable to the slope itself, this datum also suggests that $-dE_T/dT$ exceeds $E_T/T = 1160/293 \cong 4.0$, in which case S_{sc} would be positive.

Bauer and Benham (1993) proposed a novel method for estimating supercoiling free energies, enthalpies, and entropies of pBR322 by investigating the superhelix densities and temperatures at which initial melting events take place. Unlike the measurements discussed above, which pertain to DNAs at equilibrium, this method focuses on the melting behavior of DNAs that are undergoing gel electrophoresis. In addition, several explicit and implicit assumptions of uncertain validity are required to interpret the data. These assumptions are enumerated and critiqued in Appendix A. For reasons indicated therein, the best-fit free energy, enthalpy, and entropy of supercoiling obtained by Bauer and Benham's method are judged to be not as reliable quantitatively as the results of direct calorimetry or topoisomer distribution experiments, and are not directly compared with the simulations in the present work. Nevertheless, for reference, the results of Bauer and Benham (1993) imply that $E_T = 1200$ and $dE_T/dT = -10.1\ K^{-1}$ for pBR322 at 310 K. These values are significantly smaller than those obtained from topoisomer distributions of pBR322 at different temperatures by Duguet (1993), but the $-dE_T/dT$ significantly exceeds that reported by Seidl and Hinz (1984), so their results are intermediate between the two experiments with which our simulations are directly compared.

In summary, simulations that employ T-independent values of the twisting and bending rigidities and of the effective hard-cylinder diameter do not predict a sufficiently steep decline of E_T with increasing temperature in comparison to experiment. Consequently, there must be some as yet unknown temperature dependence and concomitant positive entropic contribution of one or more of these input parameters.

The objective of this paper is to investigate the origin of the temperature dependence of the experimental supercoiling free energy. To illustrate the problem, a 1515-bp model DNA is simulated using a T-invariant bending rigidity corresponding to a persistence length, $P = 500$ Å; a T-invariant torsional rigidity, $C = 3.0 \times 10^{-19}$ dyne cm^2; and a T-invariant hard-cylinder diameter, $d = 61.9$ Å, which is appropriate for the ionic conditions (30 mM KCl, 5.5 mM $MgCl_2$, 30 mM Tris) in Duguet's experiments. The simulated E_T values are then contrasted with the relevant experimental data of Duguet (1993). Then the torsional rigidity of an 1876-bp restriction fragment of pBR322 is measured by time-resolved fluorescence polarization anisotropy (FPA) over the temperature interval 278–323 K in Duguet's buffer and is found to decrease substantially with increasing T. Finally, a 4349-bp model DNA is simulated over a range of temperatures using $P = 500$ Å, $d = 61.9$ Å, and the appropriate value of the measured temperature-dependent torsional rigidity at each temperature. The predicted slope, dE_T/dT, agrees with the experimental slope from microcalorimetry (Seidl and Hinz, 1984), but significantly underestimates that reported for pBR322 by Duguet (1993).

MATERIALS AND METHODS

Sample preparation

Multiple crude extracts of pBR322 were isolated from *Escherichia coli* HB101 cells harboring the plasmid. The protocol for cell growth, harvesting, and lysis, as well as the plasmid isolation procedure, were described previously (Kim, 1993). After the phenol/ether extraction procedure to remove cellular proteins, the sample was dialyzed for 12 h against 6 liters of high-salt buffer (500 mM NaCl, 10 mM Tris, 1 mM Na_2EDTA, pH 8.5) and for 24 h against 6 liters of low-salt buffer (10 mM NaCl, 10 mM Tris, 1 mM Na_2EDTA, pH 8.5), all at 4°C. This cycle was repeated twice more to ensure removal of excess diethyl ether.

High-performance liquid chromatography (HPLC) purification of the supercoiled (SC) form of pBR322 was performed using a Macherey-Nagel Nucleogen DEAE 4000-7 IWC anion exchange column in line with a universal guard column cartridge holder containing a Microsphere 300-Å wax 7-μm guard cartridge (all purchased from Alltech Associates). The particular protocol for this separation is described elsewhere (Delrow, 1996). The pBR322 sample eluting at ~0.75 M KCl was greater than 98% supercoiled, as determined by gel electrophoresis. The supercoiled plasmid fractions from multiple HPLC runs were pooled together and dialyzed exhaustively in STE buffer (100 mM NaCl, 10 mM Tris, 1 mM Na_2EDTA, pH 8.5) at 4°C to remove the urea from the sample.

It was decided to measure the torsion constant versus temperature of the 1876-bp *Hae*II restriction fragment of pBR322, which extends from position 2719 clockwise around the origin to position 232, instead of the whole linearized plasmid (4363 bp), for two reasons. First, it was hoped that the very long times (several weeks) required to equilibrate metastable secondary structures in the whole linearized plasmid would be considerably reduced in this shorter restriction fragment. Second, the present FPA measurements are part of a larger and much more detailed study of secondary structure equilibria in different DNAs. Dynamic light scattering (DLS) measurements at large scattering vectors, which were performed in that study, are relatively more sensitive to changes in the dynamic bending rigidity and less sensitive to changes in the torsional rigidity, for an 1876-bp DNA than for a 4363-bp DNA. Thus they provide more robust information about any changes in dynamic bending rigidity in the case of the 1876-bp fragment. Because accurate information regarding any changes in torsional rigidity is already available from FPA measurements, it was desired to maximize the information from DLS pertaining to the dynamic bending rigidity, which meant preparing and studying the shorter fragment.

The 1876-bp fragment was generated by cutting the purified pBR322 with *Hae*II endonuclease, which was subsequently removed by the standard phenol/ether extraction procedure, followed by the high/low-salt dialysis treatment mentioned above. Isolation of the 1876-bp fragment was accomplished by utilizing the same Macherey-Nagel Nucleogen 4000-7 IWC anion exchange column as was used in the SC plasmid purification procedure. The particular protocol for this purification is also described elsewhere (Delrow, 1996). Multiple passes eventually achieved an adequate separation of the 1876-bp fragment from its complementary fragment, and produced a sample purity greater than 98%, as determined by gel electrophoresis. This sample was dialyzed into, and stored in, STE buffer

at 4°C. Immediately before study, this sample was dialyzed into the same buffer (5.5 mM $MgCl_2$, 30 mM KCl, 30 mM Tris, pH 7.8) that was employed in the topoisomerization experiments of Duguet (1993). All samples exhibited $A_{260}/A_{280} \geq 1.9$. DNA concentrations were determined from A_{260} measurements by assuming that an A_{260} of 20 corresponds to 1 mg/ml DNA.

Fluorescence polarization anisotropy measurements

The instrumentation and protocols used in the FPA measurements were reviewed previously (Schurr et al., 1992; Heath et al., 1996; Gebe et al., 1996). All measurements were performed on the 1876-bp linear DNA in Duguet's buffer. Temperatures were adjusted by using a temperature-controlled water circulator connected to a circulating block that holds the sample cuvette. All samples contained 0.4 ml of solution with ~50 μg/ml DNA. The extrinsic probe, ethidium, was present at a total concentration of 1 dye/300 bp.

Each sample was illuminated with ~15-ps pulses of polarized 575-nm light, and the parallel ($I_{\|}(t)$) and perpendicular ($I_{\perp}(t)$) components of the subsequent emission were detected at 640 nm. The width (FWHM) of the instrument function ($e(t)$) in these studies was 60–70 ps. The emission intensities were combined to yield the total fluorescence decay, ($s(t) = i_{\|}(t) + 2i_{\perp}(t)$, and the difference decay, $d(t) = i_{\|}(T) - i_{\perp}(t)$, which are convolutions of, respectively, the true sum response functions $S(t)$ or true difference response function, $D(t)$, with $e(t)$. Adjustable parameters in the theoretical model functions for $S(t)$ and $D(t)$ were determined from $s(t)$, $d(t)$, and $e(t)$ using least-squares convolute and compare algorithms. $S(t)$ is modeled by a sum of two exponentials plus a delta function to account for Raman scattered light. Under the present conditions, the dominant exponential component has a lifetime of 22(± 1) ns, corresponding to intercalated dye, whereas the minor component has a lifetime of (1.5–2) ns, corresponding to nonintercalated dye. The first three nanoseconds of data after the excitation pulse were excluded from fits of the difference data to eliminate any contribution of nonintercalated ethidium. In that case, the true difference function can be modeled by $D(t) = r(t)S(t)$, wherein the theoretical anisotropy function is given by

$$r(t) = r_0 \sum_{n=0}^{2} I_n C_n(t) F_n(t) \qquad (4)$$

The adjustable initial anisotropy r_0 accounts for isotropic local angular motions that are too rapid to resolve (Schurr and Fujimoto, 1988; Schurr et al., 1992). The twisting correlation functions are given by (Barkley and Zimm, 1979; Allison and Schurr, 1979)

$$C_n(t) = \exp[-n^2 k_B T(\pi\alpha\gamma)^{-1/2} t^{1/2}] \qquad (5)$$

where α is the adjustable torsion constant between base pairs, $\gamma = 4\pi a^2 h\eta$ is the friction factor for azimuthal rotation around the symmetry axis, h = 3.4 Å is the rise per base pair, a = 12 Å is the hydrodynamic radius for long DNAs (Wu et al., 1987), and η is the solvent viscosity. The appropriate temperature and solvent viscosity were employed in each case. The tumbling correlation function is taken to be $F_n(t) = 1.0$, which corresponds to a dynamic persistence length, $P_d = \infty$. The I_n are well-known trigonometric functions: $I_0 = [\frac{1}{2}\cos^2\epsilon - \frac{1}{2}]^2$, $I_1 = 3\cos^2\epsilon \sin^2\epsilon$, and $I_2 = (\frac{3}{4})\sin^4\epsilon$, where $\epsilon = 70.5°$ is the polar angle between the helix-axis and the transition dipole. Fits of the theory to the difference data, using r_0 and α as adjustable parameters, were rather good, with reduced χ^2 values less than 1.10 in most cases. At every temperature, the variation of the best-fit torsion constant with the time span of the fitted data is similar to that in Fig. 1, which applies for 37°C. For unknown reasons, possibly related to excess scattering, the first point (0–18 ns) is always somewhat higher than the others, and its standard deviation is also much greater. This effect, which is peculiar to this study, is believed to be spurious. In any case, the best-fit torsion constants from the two longest time spans (0–69 and 0–119 ns) were averaged to yield a single value, which was then multiplied by the factor 1.35 to correct from the assumed $P_d = \infty$ to our current best guess, P_d = 1500 Å (Fujimoto and Schurr, 1990; Schurr et al., 1992; Hustedt et al., 1993; Reese, 1996). The resulting values are referred to as corrected average torsion constants ($\langle\alpha\rangle$). Measurements were performed in the sequence 293, 310, 323, and 333 K, allowing at least 6 h of equilibration time after reaching each temperature. This DNA sample in Duguet's buffer showed signs of substantial aggregation at 333 K, as expected in the presence of 5.5 mM Mg^{2+}, and upon returning to 293 K did not reproduce the original torsion constant at that temperature. Consequently, the 333 K data were disregarded. A new sample was prepared and measured at 293 K and 278 K. Its value at 293 K was within experimental error the same as that of the original sample. Similar FPA measurements were performed in Duguet's buffer without the 5.5 mM $MgCl_2$, and in the STE buffer, which has no Mg^{2+}. Throughout this series of measurements, the samples were stored at 4°C overnight.

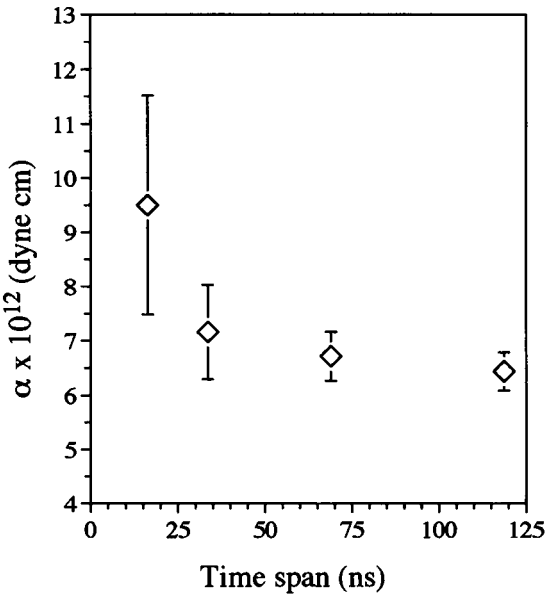

FIGURE 1 Best-fit torsion constant, α, versus time span of the fitted data for the 1876-bp fragment. Measurements were performed in Duguet's buffer (5.5 mM $MgCl_2$, 30 mM KCl, 30 mM Tris, pH 7.8) at 20°C.

Simulation model and basic theory

The closed circular DNA is modeled as a chain of N contiguous subunits, each of which has a length b and is connected to its adjoining neighbors by Hookean bending and twisting springs. The subunits are labeled by the index j, where j = 1, 2, 3, . . . , N. Embedded in the jth subunit is a coordinate frame, which is chosen so that the z_j axis lies along the bond vector ($\mathbf{b}_j$) from the jth to (j + 1)th subunit. The Euler rotation that carries a coordinate frame from coincidence with the laboratory frame (x', y', z') to coincidence with the jth frame is $\Phi_j = (\alpha_j, \beta_j, \gamma_j)$, where the angles pertain to successive rotations around the body-fixed z', y'', and z''' axes. Here, z' coincides with the laboratory z' axis, y'' is the y axis of the rotating frame after rotation by α_j around z', and z''' is the z axis of the rotating frame after the further rotation by β_j around y'', so z''' corresponds to z_j. The Euler rotation that orients the (j + 1)th frame in the jth frame is $\Phi_{j,j+1} = (\alpha_{j,j+1}, \beta_{j,j+1}, \gamma_{j,j+1})$. In either case, the allowed ranges of these angles for geometrical purposes are $0 \leq \alpha \leq 2\pi$, $0 \leq \beta \leq 2\pi$, and $0 \leq \gamma \leq 2\pi$, but when the potential energy is evaluated, the allowed ranges are taken as $-\pi \leq \alpha \leq \pi$, $0 \leq \beta \leq \pi$, $-\pi \leq \gamma \leq \pi$. The bending angle between the z_j axis of the jth subunit and the z_{j+1} axis of the (j + 1)th subunit is $\beta_{j,j+1}$.

The net twist experienced by a coordinate frame as it undergoes the Euler rotation $\Phi_{j,j+1}$ from the jth to the $(j+1)$th frame is $\phi_{j,j+1} = \alpha_{j,j+1} + \gamma_{j,j+1}$.

The total potential energy of a given configuration is assumed to be

$$U_{tot} = U_b + U_t + U_I \tag{6}$$

wherein U_b is the bending potential energy, U_t is the twisting potential energy, and U_I is the potential energy due to intersubunit interactions besides those ascribed to twisting and bending. Because one or more of these potential energies may be temperature dependent for a fixed molecular configuration, they should properly be regarded as potentials of mean force (i.e., free energies at fixed values of the relevant intersubunit coordinates), rather than pure potential energies. The model filament is assumed to have an isotropic bending potential with no permanent bends, and the intersubunit interaction is assumed to be invariant to azimuthal rotation of each of the interacting subunits around its own z_j axis. For such a model, local fluctuations in twist about the uniform net twist per subunit always make the same contribution to the configuration integral and to the relative probabilities of different configurations, and can therefore be omitted (Gebe et al., 1995). Consequently, the relevant twisting potential energy for these simulations is just the reduced potential energy associated with the uniform net twist,

$$U_t^{red} = (\alpha(2\pi)^2/2N)(\Delta l - w)^2 \tag{7}$$

wherein $\alpha = C/|\mathbf{b}|$ is the torsion constant of the intersubunit torsion spring, and the writhe (w) is given by

$$w = \frac{1}{4\pi}\sum_{\substack{i=1\\ i\neq j}}^{N}\sum_{j=1}^{N}\frac{(\mathbf{b}_i \times \mathbf{e}_{ij}\cdot\mathbf{b}_j)}{|\mathbf{r}_j - \mathbf{r}_i|^2} \tag{8}$$

where $\mathbf{e}_{ij} = \mathbf{r}_{ij}/|\mathbf{r}_{ij}|$ is a unit vector along $\mathbf{r}_{ij} = \mathbf{r}_i - \mathbf{r}_j$. In deriving Eq. 7, use is made of the topological constraint, $\Delta l = l - l_0 = t - l_0 + w$, which applies to all circular DNAs. The uniform net twist (beyond l_0) is $t - l_0 = \Delta l - w$. The bending potential energy is

$$U_b = \frac{\kappa_\beta}{2}\sum_{j=1}^{N}\beta_{j,j+1}^2 = \frac{\kappa_\beta}{2}\sum_{j=1}^{N}[\arccos((\mathbf{b}_{j+1}\cdot\mathbf{b}_j)/b^2)]^2 \tag{9}$$

where κ_β is the bending constant of the intersubunit bending spring. The subunit interaction energy, U_I, is taken to be a hard cylinder potential, which is either infinite or zero, depending on the separation of the cylinders. The protocol for evaluating this interaction was presented previously (Gebe et al., 1995).

Simulation protocol

The simulation algorithm used herein was introduced by Gebe et al. (1995) and is described briefly as follows. Very small random rotations, δx_j, δy_j, δz_j, of each subunit around its three body-fixed axes are performed for every subunit in the chain at the same time. This $3N$-fold rotation constitutes a single move. The Euler angles that orient each subunit in the laboratory frame are updated by using the linear small angle relations (Gebe et al., 1995). The new set of bond vectors $\{\mathbf{b}_1, \mathbf{b}_2, \ldots, \mathbf{b}_n\}$ is then calculated from the new set of angles $\{\alpha_1, \beta_1; \alpha_2, \beta_2; \ldots; \alpha_N, \beta_N\}$ and summed to yield the offset vector, $\mathbf{r}_N = \sum_{j=1}^{N}\mathbf{b}_j$, which must vanish for a circular array. Using the correction algorithm described by Gebe et al. (1995), this offset vector is apportioned among the N bond vectors by subtracting from each a small perpendicular vector, which is proportional to the projection of $\mathbf{r}_N$ onto the plane perpendicular to that bond vector, while maintaining a constant bond vector length. The corrected bond vectors are used to calculate the subunit positions, $\mathbf{R}_j = \sum_{i=1}^{j-1}\mathbf{b}_i$, and to recalculate the polar angles, $\alpha_i\beta_i$, of each bond vector in the laboratory frame. The hard cylinder potential is then evaluated. If that is finite, then the reduced potential energy of the new configuration is evaluated, and the Metropolis criterion is applied to either provisionally accept the new configuration or reject it in favor of the old. Each provisionally kept configuration is further examined for possible changes in knot topology by calculating its Alexander polynomial (Frank-Kamenetskii and Vologodskii, 1981). If such a change in knot topology has occurred, the new configuration is rejected in favor of the old, and if not it is finally accepted.

Free energy of supercoiling and the twist energy parameter

At constant temperature and pressure, the supercoiling free energy is given by

$$dG_{sc} = \delta w_{sc} \tag{10}$$

where δw_{sc} is the non-pressure-volume work needed to increase the linking difference by $d(\Delta l)$. This work is $d(\Delta l)$ times the opposing torque that resists the increase in linking difference, $\langle \partial U_{rc}/\partial(\Delta l)\rangle$, where the angle brackets $\langle\rangle$ denote an equilibrium ensemble average. This free energy change can therefore be written as

$$dG_{sc} = \left\langle\frac{\partial U_{rc}}{\partial(\Delta l)}\right\rangle d(\Delta l) = \frac{(2\pi)^2\alpha}{N}(\Delta l - \langle w\rangle)d(\Delta l) \tag{11}$$

wherein $\langle w\rangle$ is the ensemble average writhe. The free energy change accompanying the introduction of linking difference Δl into the DNA can be determined by numerical evaluation of the integral,

$$\Delta G_{sc}(\Delta l) = \left(\frac{(2\pi)^2\alpha}{N}\right)\int_0^{\Delta l}(\Delta l' - \langle w\rangle)d(\Delta l') \tag{12}$$

In fact, for DNAs with $N \geq 4000$ bp, both $\langle w\rangle$ and the integrand in Eq. 12 are practically proportional to $\Delta l'$, so the numerical integration is unusually straightforward. E_T can then be determined from $\Delta G_{sc}(\Delta l)$ and Δl by using Eq. 11 in the form

$$E_T = N\Delta G_{sc}(\Delta l)/(k_B T \Delta l^2) \tag{13}$$

Simulation parameters

Monte Carlo simulations were performed on closed circular DNAs containing $N = 54$ subunits (1515 bp) and $N = 155$ subunits (4349 bp). In both cases the subunit length was $b = 95.4$ Å. Simulations were performed at $\Delta l = 0.75$, 1.50, and 2.25 turns for the 1515-bp DNA, and at $\Delta l = 2.00$ and 4.00 turns for the 4349-bp DNA. Both DNAs were simulated over a temperature range of 278–358 K. The solution surrounding the simulated DNA was assumed to be 5.5 mM $MgCl_2$, 30 mM KCl, and 30 mM Tris, which matches the experimental conditions of Duguet, and the value of the effective hard-cylinder diameter, $d_B = 61.9$ Å, was determined for this set of ionic conditions at $T = 298$ K. This was done by first solving the nonlinear Poisson-Boltzmann (NLPB) equation for a cylinder with a 12-Å radius and the linear charge density of DNA immersed in the mixed-valence electrolyte (Delrow et al., 1997), and then following the protocol of Stigter (1977) to determine 1) the particular solution of the linearized Poisson-Boltzmann (LPB) equation that matches the NLPB solution at large distances, 2) the second virial coefficient for line charges interacting according to that LPB potential, and 3) the effective hard-cylinder diameter that yields the same second virial coefficient. Neither the NLPB nor the LPB solutions vary significantly with T, because they depend only on the product $\epsilon k_B T$, where ϵ is the dielectric constant, and this product is practically invariant to T over the range considered. Consequently, d_b is likewise invariant to T over that same range.

Each simulation of the 1515-bp DNA consisted of 3 million ($3N$-fold) moves, and in the case of the 4349-bp DNA consisted of 10 million moves. In all simulations, 45–55% of the configurations were accepted. All sim-

ulations were performed on IBM RISC 6000 computers (either model 350 or model 580).

Elastic constants for bending and torsion

In all cases, the bending spring constant, κ_β, was chosen such that the intrinsic persistence length was P = 500 Å, independent of T. The T-invariant torsion spring constant between base pairs was fixed at $\alpha = 8.8 \times 10^{-12}$ dyne cm, which is equivalent to a torsional rigidity, $C = 3.0 \times 10^{-19}$ dyne cm^2. The T-invariant torsion spring constant between the longer (28 bp) subunits of the simulation model was chosen to yield precisely the same torsional rigidity. This assumed C value corresponds nearly to the largest reported values, which are found only for small circular DNAs that contain $N \leq 250$ bp (Heath et al., 1996). It is chosen here to provide the highest possible E_T values for comparison with pBR322, which exhibits anomalously large E_T values, as noted above.

T-dependent torsion constants were obtained from the present FPA measurements of ethidium bromide intercalated in the 1876-bp *Hae*II restriction fragment of pBR322 DNA (cf. Fig. 2). Averaged values of the measured torsion constant between base pairs, $\langle\alpha\rangle$, were scaled to yield the same torsional rigidities for the model of longer subunits and used for simulations at 278, 293, 310, and 323 K. Simulations at higher temperatures used values extrapolated from the weighted least-squares fit of a straight line to the $\langle\alpha\rangle$ versus T data.

RESULTS AND DISCUSSION

Illustration of the problem

Simulated E_T values for a model 1515-bp DNA with T-invariant torsional rigidity, bending rigidity, and hard-cylinder diameter are coplotted with the experimental data of Duguet (1993) versus T in Fig. 2. Obviously, the slope, $-dE_T/dT = (15.6 \pm 1)\ K^{-1}$, of the experimental data substantially exceeds that of the simulated data, $-dE_T/dT = (4.0 \pm 0.5)\ K^{-1}$, for this model with a T-invariant potential surface. The experimental slope implied by the microcalorimetry data of Seidl and Hinz (1984), namely $-dE_T/dT = (8.6 \pm 1.6)\ K^{-1}$, likewise substantially exceeds this simulated value. Moreover, the simulated slope lies slightly below the value $E_T/T = 1475/310 = 4.8$ at 310 K, so according to Eq. 3 the supercoiling entropy is small and negative, whereas the experimental estimates are both large and positive, as noted previously (Vologodskii and Cozzarelli, 1994). Clearly, the simulated E_T values for a model DNA with a T-invariant potential energy surface do not decline sufficiently rapidly with increasing T to match the slopes of the experimental data.

Temperature dependence of the torsion elastic constant

Corrected average torsion constants ($\langle\alpha\rangle$) between base pairs of the 1876-bp DNA in the different buffers are plotted versus T in Fig. 3. A significant decline in $\langle\alpha\rangle$ with increasing T is readily apparent.

When the 5.5 mM $MgCl_2$ is removed from Duguet's buffer, the $\langle\alpha\rangle$ values are significantly lower (by ~20–30%), but the negative slope, $d\langle\alpha\rangle/dT$, remains similar to that in the presence of $MgCl_2$. When the buffer is changed to STE, the entire $\langle\alpha\rangle$ versus T curve, including the slope, is similar to that in Duguet's buffer without the 5.5 mM $MgCl_2$. For this 1876-bp fragment in the buffers without

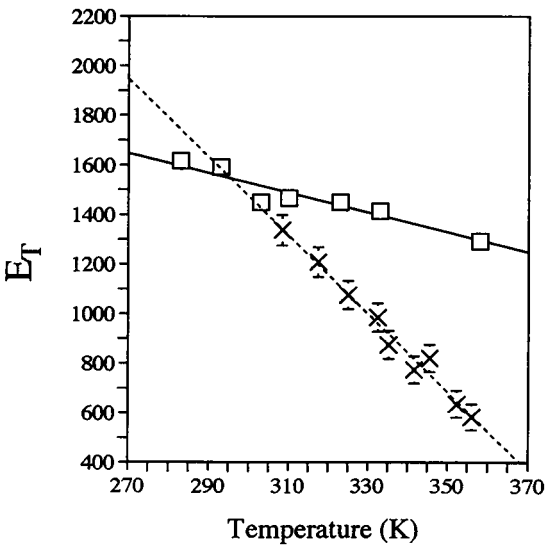

FIGURE 2 Twist energy parameter, E_T, versus temperature. Data are from Duguet's experiments on pBR322 (×) and our simulations of a 1515-bp closed circular DNA (□). The dashed and solid lines represent the weighted least-squares fit of the experimental and simulated data, respectively. Simulations employed T-independent bending, twisting, and interaction potentials. Simulation parameters: persistence length P_L = 500 Å; torsional rigidity $C = 3.0 \times 10^{-19}$ dyne cm^2; equivalent hard-cylinder diameter d_B = 61.9 Å.

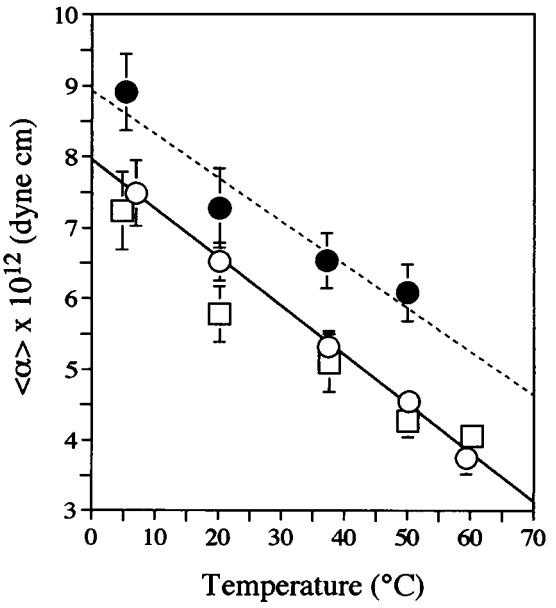

FIGURE 3 The average torsion constant, $\langle\alpha\rangle$, versus temperature for an 1876-bp restriction fragment of pBR322. The DNA is present in Duguet's buffer (5.5 mM $MgCl_2$, 30 mM KCl, 30 mM Tris, pH 7.8) at 20°C (●); Duguet's buffer without the 5.5 mM $MgCl_2$ at 20°C (○); and STE buffer (0.1 M NaCl, 10 mM Tris, 1 mM EDTA, pH 8.5) at 20°C (□). The dashed and solid lines represent least-squares fits to the data collected in Duguet's buffer with and without 5.5 mM $MgCl_2$, respectively.

Mg^{2+} ions, the torsion constant at 20°C lies in the range $(5.8-6.5) \times 10^{-10}$ dyne cm, which is typical of measurements on linearized pBR322 (Fujimoto and Schurr, 1990; Schurr et al., 1992). In addition, two other DNAs, namely a 1764-bp restriction fragment from p30δ and the linearized replicative form (RF) of M13mp8, both in Duguet's buffer without the 5.5 mM $MgCl_2$, exhibited slopes of $\langle\alpha\rangle$ versus T similar to those of the present 1876-bp fragment (Delrow et al., manuscript in preparation). For all three of these DNAs, the negative slope, $d\langle\alpha\rangle/dT$, is a more or less universal property.

The present results contrast sharply with those previously reported for ϕ29 DNA (Thomas and Schurr, 1983; Wilcoxon and Schurr, 1983) and chicken erythrocyte DNA (Robinson et al., 1980), which exhibit torsional rigidities that are practically independent of T from 0°C to the melting region. This difference is tentatively ascribed to differences in sequence. It is noteworthy that ϕ29 and certain other DNAs exhibit a considerably (~25%) smaller torsion constant at 293 K than either pBR322 or its 1876-bp subfragment (Schurr et al., 1992), which implies that a different average secondary structure prevails in ϕ29 than in the 1876-bp DNA. The present results suggest that the prevailing equilibrium among secondary structures is more evenly balanced, and therefore more sensitive to temperature, in the 1876-bp subfragment of pBR322 than in ϕ29 DNA. The notion that the average secondary structure reflects a sequence-dependent and T-dependent equilibrium between different states with different torsional rigidities has some precedent. Strong evidence for a substantial effect of temperature on the structural equilibria and flexibility of duplexes containing poly dA · poly dT and phased oligo dA · oligo dT tracts was reported by Chan et al. (1990, 1993, 1997) and Herrera and Chaires (1989). Abundant evidence for a substantial and very long-range effect of a particular change in sequence (insertion of $(CG)_8$) on the average secondary structure and torsion constant of an 1100-bp sequence was reported by Kim et al. (1993). Additional physical evidence that the observed decrease in average torsion elastic constant with increasing T represents a change in secondary structure will be presented elsewhere (Delrow et al., manuscript in preparation).

Over the T range of 278–323 K, the best-fit torsion constants are largely independent of time span of the fitted data for the three longest time spans, as illustrated in Fig. 1. A significantly higher α value and a much larger standard deviation are found for the shortest time span (0–18 ns) at all temperatures examined, but this is not understood and is likely to be an artifact. The similarity of the α values for the three longest time spans at any given temperature, the relatively high values of those longest time-span data, and the invariance of the shape of the α versus time-span curves over such a wide range of temperatures all suggest that the decrease in $\langle\alpha\rangle$ with increasing T does not arise from isolated rigidity weaknesses at sites of local denaturation. The close similarity of the $\langle\alpha\rangle$ versus T curves exhibited by the present DNA in buffers of significantly different ionic strength, namely in Duguet's buffer without the $MgCl_2$ (0.04 M ionic strength) and in STE buffer (0.10 M ionic strength), also suggests that local denaturation does not contribute significantly to either $\langle\alpha\rangle$ or its decline with increasing T. In any case, the highest temperature considered (60°C) lies more than 25° below the T_m of this linear DNA, so significant local denaturation is not expected.

For completeness, we note other possible origins of the difference in $d\langle\alpha\rangle/dT$ between these (and other recent) measurements on DNAs grown in *E. coli* cells and the earlier measurements on viral ϕ29 and chicken erythrocyte DNAs (Thomas and Schurr, 1983; Wilcoxon and Schurr, 1983; Robinson et al., 1980). Some difference in the host's ability to modify the DNA, for example, by methylation, or even by maintaining a different superhelix density, might be involved. It is also conceivable that certain differences in preparation protocols, for example, the use of HPLC in the more recent studies, may have unexpected consequences. Any difference in environmental history, whether inside the host or during preparation, could in principle affect $\langle\alpha\rangle$ and $d\langle\alpha\rangle/dT$, whenever metastable states contribute significantly to the average properties. The existence of metastable secondary structure in some DNAs is well documented (Wu et al., 1988, 1991; Wu and Schurr, 1989; Song et al., 1990; Schurr et al., 1992; Naimushin et al., 1994; Heath et al., 1996) and is difficult to completely rule out for any DNA, because the relevant equilibration times are so long. Likewise, the possibility that a very small amount of tenaciously bound contaminant (e.g., a protein) substantially affects $\langle\alpha\rangle$ and $d\langle\alpha\rangle/dT$ can never be completely ruled out. Finally, the buffer in the earlier studies on ϕ29 DNA contained 20 mM Na_2EDTA instead of the 1 mM Na_2EDTA that prevails in the present STE buffer. Although such a difference in EDTA concentration has no effect on the torsional rigidities of other DNAs examined at room temperature, the possibility that it significantly affects $d\langle\alpha\rangle/dT$ cannot be excluded on the basis of existing results. Although all of these hypothetical scenarios are possible, at the present time they must be regarded as somewhat less likely origins of the difference in $d\langle\alpha\rangle/dT$ than a sequence-dependent shift in the secondary structure equilibrium. Because considerable forthcoming evidence rather strongly implicates a change in secondary structure with increasing T, one must expect some sequence dependence of such a phenomenon in any case.

Temperature dependence of E_T

Simulated E_T values for 1515-bp model DNAs with 1) a constant torsional rigidity, $C = 3.0 \times 10^{-19}$ dyne cm^2 ($\alpha = 8.8 \times 10^{-12}$ dyne cm), and 2) the measured T-dependent torsional rigidities inferred from the torsion constants in Fig. 3, are compared in Fig. 4. Use of the T-dependent torsional rigidities increases the slope, $-dE_T/dT$, by a factor of somewhat more than 2.

Simulated E_T values for the present 4349-bp model with P = 500 Å, d = 61.9 Å, and temperature-dependent tor-

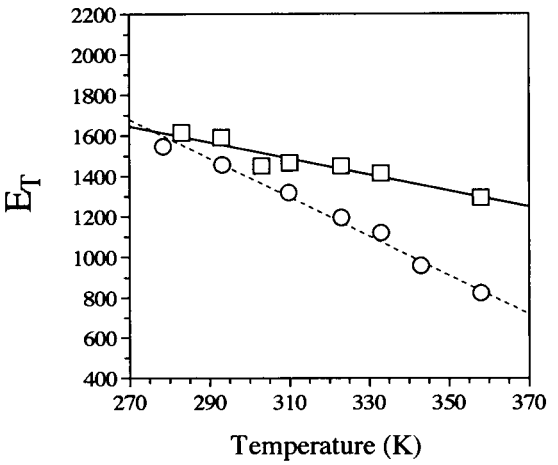

FIGURE 4 Simulated twist energy parameter, E_T, for a 1515-bp closed circular DNA versus temperature. Simulations were performed using a T-invariant torsional rigidity, $C = 3.0 \times 10^{-19}$ dyne cm^2 ($\alpha = 8.8 \times 10^{-12}$ dyne cm) (□); and the T-dependent torsion constants of the 1876-bp DNA in Duguet's buffer (*dashed line* in Fig. 3) (○). The solid and dashed lines represent least-squares fits to the simulated data for, respectively, T-invariant and T-dependent torsion constants.

sional rigidities, reckoned from the data in Fig. 2, are plotted versus T in Fig. 5. Also coplotted in the same figure is the experimental line calculated from the ΔH_{sc} measurements of Seidl and Hinz (1984) and Eq. 2, under the assumption that $E_T = 1000$ at 310 K for their ColE1 *amp* DNA. Their ΔH_{sc} measurements define the slope, $-dE_T/dT$, of that line, but its vertical height depends on the value assumed for E_T. The agreement between the simulated and experimental slopes is obviously reasonably good. Numerical values of the slopes, E_T values at 310 K, and $\Delta S_{sc}/R$ are presented in Table 1. If ColE1 *amp* DNA were to exhibit the same slope, $d\langle\alpha\rangle/dT$, of its torsion constant versus temperature as the present 1876-bp fragment of pBR322, then that would account for most of the temperature dependence of its E_T, and most of its positive ΔS_{sc}.

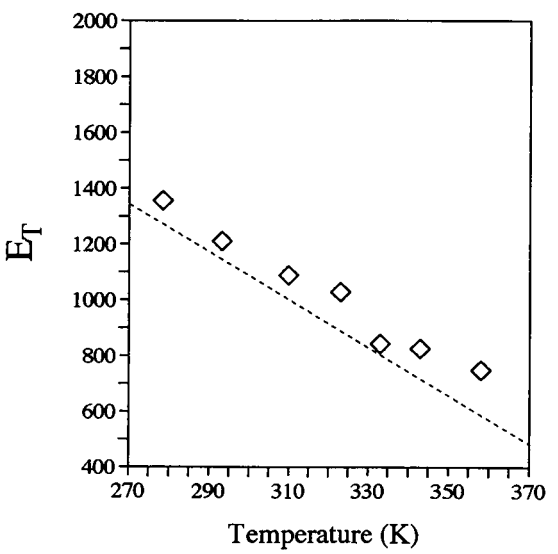

FIGURE 5 Twist energy parameter, E_T, versus temperature. Data are from simulations of a 4349-bp closed circular DNA employing T-dependent torsion constants (◇). The dashed line represents the microcalorimetric measurements for ColE1 *amp* plasmid DNA by Seidl and Hinz (see text for details). Simulation parameters: persistence length $P_L = 500$ Å; equivalent hard-cylinder diameter $d_B = 61.9$ Å.

Simulated E_T values for the present 4349-bp model with temperature-dependent torsional rigidities are coplotted with experimental data on pBR322 from Duguet (1993) and others in Fig. 6. The slope, $-dE_T/dT$, of Duguet's data exceeds that of the simulated values by more than twofold. The particular numerical values are compared in Table 1. The other experimental data in Fig. 6 lend some support to the large experimental slope manifested by Duguet's data. In the case of pBR322 the measured slope, $d\langle\alpha\rangle/dT$, of its torsion constant versus T evidently does not suffice to account for the rather large value of $-dE_T/dT$. The most likely explanation of this discrepancy is that the bending rigidity of pBR322 also decreases with increasing temperature. That is a topic for future work.

The possibility that local denaturation contributes significantly to $-dE_T/dT$ in the experiments of Duguet (1993) is tentatively discounted for the following reasons.

1. All of Duguet's data apply for superhelix densities that lie well below the thresholds for local denaturation of pBR322 at all temperatures examined, even in solutions of much lower ionic strength (0.01 M) (Kowalski et al., 1988; Benham, 1992; Bauer and Benham, 1993). Indeed, the superhelix densities in Duguet's experiments lie within the realm of thermally accessible fluctuations, and sample no more torsionally strained states than are sampled by the FPA measurements of $\langle\alpha\rangle$. As noted above, there is no indication that local denaturation contributes significantly to $\langle\alpha\rangle$ or $d\langle\alpha\rangle/dT$.

2. If local denaturation were to contribute substantially to E_T and $-dE_T/dT$, as determined from topoisomer distribution experiments, then in any measurement of the relative populations of thermally accessible topoisomers one would expect to find that E_T was significantly larger for positively supercoiled than for negatively supercoiled topoisomers. That would result in a marked asymmetry of the population

TABLE 1 Twist energy parameter (E_T), slope ($-dE_T/dT$), and entropy of supercoiling (ΔS_{sc}) for pBR322

Study	E_T*	$-dE_T/dT$ (K^{-1})	$\Delta S_{sc}/R$
Theory	1090 ± 100	7.6 ± 1[#]	1266 $\Delta\ell^2/N$[§]
Seidl and Hinz	1000[¶]	8.6 ± 1[‖]	1666 $\Delta\ell^2/N$[§]
Duguet	1320 ± 130	15.6 ± 1	3485 $\Delta\ell^2/N$[§]
Horowitz and Wang	1130 ± 110	—	—
Naimushin et al.	1155 ± 100	11 ± 8	—

*Taken at 310 K (37°C), except for Duguet's value, which is at 308 K.
[#]Results of present simulations, using torsion constants from Fig. 5.
[§]Calculated using Eq. 3.
[¶]Supercoiling free energy is assumed to be $\Delta G_{sc}/RT = 1000\ \Delta\ell^2/N$.
[‖]Calculated from ΔH_{sc} via Eq. 2.

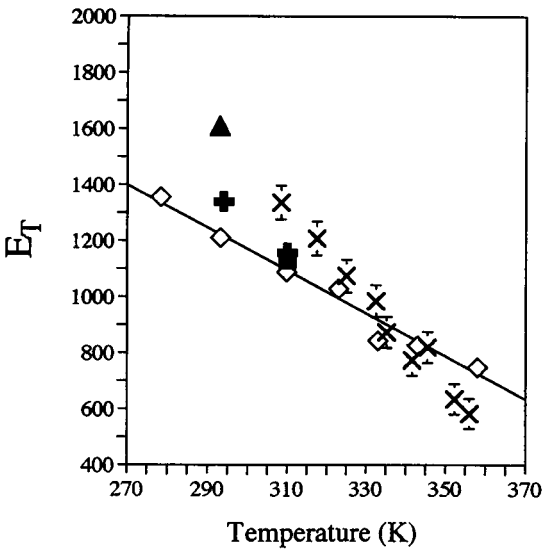

FIGURE 6 Twist energy parameter, E_T, versus temperature. Data are from simulations and experiments. The solid line represents the weighted least-squares fit of data from simulations of a 4349-bp closed circular DNA (◇) employing T-dependent torsion constants. The experimental data are from the topoisomer distribution analyses of pBR322 by Duguet (×), Naimushin et al. (+), Shore and Baldwin (▲), and Horowitz and Wang (■). Simulation parameters: persistence length P_L = 500 Å; equivalent hard-cylinder diameter d_B = 61.9 Å.

distributions. However, Duguet (1993) reported no such asymmetry, even at the highest temperatures examined.

3. There is some indication that the slope, $-dE_T/dT$, observed by Duguet for $T \geq 308$ K may also extend down to 293 K (cf. datum of Shore and Baldwin in Fig. 6 and data of Naimushin et al. in Table 1 and Fig. 6). At the relevant ionic strengths and near-zero superhelix densities of those measurements, local denaturation cannot make a significant contribution at such low temperatures.

Possible molecular origins of the T dependence of the torsion elastic constant

The preceding results establish that the large positive slope, $-dE_T/dT$, and positive entropy of supercoiling arise at least in part from the substantial negative slope, $d\langle\alpha\rangle/dT$, of the torsion constant of such a plasmid DNA, but provide no insight into the molecular origins of that. Models for the T dependence of $\langle\alpha\rangle$ fall into two classes that are not mutually exclusive. In the first class, the secondary structure is characteristic of a single free energy basin throughout the T range investigated, and the torsion constant for twisting displacements within that basin decreases with increasing temperature. For example, if twisting were accompanied by a loss of bound water, as has been suggested (Vologodskii and Cozzarelli, 1994), that would yield a positive entropy of twisting and a decrease in $\langle\alpha\rangle$ with increasing T. However, any single-basin model is difficult to reconcile with the fact that some DNAs, such as ϕ29 and chicken red cell DNA, exhibit a torsion constant that is practically independent of T (Thomas and Schurr, 1983; Wilcoxon and Schurr, 1983; Robinson et al., 1980), whereas others exhibit a substantial negative slope, $d\langle\alpha\rangle/dT$. Because the different DNAs evidently do not all reside in identical free-energy basins, different sequences in the same DNA presumably also do not reside in identical free-energy basins. A further difficulty with any solvent release explanation for the negative slope, $d\langle\alpha\rangle/dT$, is as follows. For a chiral molecule such as DNA, it is not generally expected that the twist coordinate corresponding to the minimum potential of mean force will even approximately match that for maximum solvent binding. If these two twist coordinates do not match, then twisting in one direction from the potential minimum will be accompanied by loss of bound water, but twisting in the other will be accompanied by a corresponding gain of bound water. To the extent that asymmetrical release or absorption of bound water makes a substantial contribution to the torsion potential of mean force for small thermal deformations, such as are involved in topoisomer distribution or FPA experiments, one would expect a substantial asymmetry of that torsion potential that is not observed (Selvin et al., 1991). In the unlikely event that the torsion potential remains symmetrical despite an asymmetrical loss or gain of bound water, then the contributions of the losses and gains in bound water to the twisting entropy would largely cancel in any experiment in which $\langle\alpha\rangle$ is assessed by sampling fluctuations in twist of either sign with equal probability, as is done in FPA experiments. Thus the negative slope, $d\langle\alpha\rangle/dT$, observed in the present FPA experiments is most unlikely to arise from loss of bound water upon twisting of the DNA. In the second class of model, every subunit of the DNA can exhibit either of two or more different secondary structures, each of which "occupies" a distinct free energy basin and coexists in "chemical" equilibrium with the other possible structures. Each structure is characterized by its particular intrinsic twist, which corresponds to the twist coordinate at the minimum free energy in that basin, and by its particular torsion constant for twisting displacements away from that minimum free energy position. In this model, the torsion constants of the different structures, or free energy basins, could in principle be independent of temperature. Then the T dependence of the effective torsion constant would arise entirely from the T-induced shift of subunit populations between the different free energy basins, or secondary structures.

The observed slow equilibrations of metastable secondary structures subsequent to various perturbations, including changes in superhelix density (Shibata et al., 1984; Wu et al., 1988, 1991; Wu and Schurr, 1989; Song et al., 1990; Naimushin et al., 1994), a change in T (Kim et al., 1993), ethidium binding to a particular DNA under high salt conditions (Kim et al., 1993), and bending into a small circle (Heath et al., 1996) strongly suggest the involvement of different free energy basins that are separated, at least in some cases, by significant free energy barriers. Recent physical evidence also indicates that a change in the average secondary structure of linearized plasmid DNAs, including

the present fragment, accompanies the decline in their torsion constants with increasing T (Delrow et al., manuscript in preparation). The fact that $\langle\alpha\rangle$ declines substantially with T for some DNAs, including those discussed here, but remains constant for other DNAs (Thomas and Schurr, 1983; Wilcoxon and Schurr, 1983; Robinson et al., 1980), although difficult to reconcile with any model involving a single free energy basin, could be reconciled with a model involving multiple free energy basins or states, as described below. The effect of 5.5 mM $MgCl_2$ to increase $\langle\alpha\rangle$ by 20–30% could similarly be attributed to a Mg^{2+}-induced shift of subunit populations between the different basins. The available evidence thus favors the second class of models.

A thermodynamic analysis of the twisting of a simple two-state version of the second class of models in the small deformation limit is presented in Appendix B. In this model each subunit in a chain of N such subunits can exist in either of two states, A or B, and the reaction, A $\rightleftharpoons$ B, at each subunit has an unperturbed equilibrium constant $K = f_B^\circ/f_A^\circ = \exp[-(\Delta H^\circ - T\Delta S^\circ)/k_BT]$, where f_A° and f_B° are the unperturbed fractional populations, and ΔH° and ΔS° are the standard state enthalpy and entropy differences between the A and B states (or free energy basins). The A state has intrinsic twist ϕ_A° and torsion constant $\alpha_A = g_A$, whereas the B state has the corresponding quantities ϕ_B° and $\alpha_B = g_B$, all of which are independent of T. This model has several interesting features, some of which are rather unusual, as noted below.

1. The effective force constant for twisting the entire chain (along the minimum free energy path) varies with T, and the total twisting entropy, ΔS, is proportional to ΔH° (but not to ΔS°) of the chemical reaction. In this case, the entropy change upon twisting arises entirely from relative changes in the fractional populations of the two states. ΔH° merely determines the direction and steepness of this change with increasing T. Thus it is not necessary to postulate a loss of bound water or any other species to explain a nonvanishing entropy of twisting, when this model applies.

2. The shift of the chemical equilibrium upon twisting, as manifested by the change (δf_B) in fractional occupation of the B state, may exhibit either of two rather different kinds of behavior in different limits. 1) When $g_A = g_B$, but $\phi_A^\circ \neq \phi_B^\circ$, then δf_B is proportional to the net twist per subunit ($\Delta t/N$) to lowest order in $\Delta t/N$. In this limit, the shift in the chemical equilibrium contributes to a $N(\Delta t/N)^2$ term in the total free energy of twisting, and therefore contributes directly to the effective force constant for twisting, which is then lower than it would be if the reaction were "frozen." 2) When $\phi_A^\circ - \phi_B^\circ = 0$, but $g_A \neq g_B$, then δf_B varies as $(\Delta t/N)^2$ (instead of $\Delta t/N$) to lowest order. In this limit, the shift in the chemical equilibrium contributes to ΔG_{tot}^{min} only a term proportional to $N(\Delta t/N)^4$ in lowest order, which is negligibly small compared to the $N(\Delta t/N)^2$ term. Consequently, the chemical equilibrium has no significant influence on the effective force constant for twisting, which is precisely the same as for a chain of subunits in which the chemical equilibrium is "frozen" at its equilibrium position.

3. In the limit when $\phi_A^\circ = \phi_B^\circ$, but $g_A \neq g_B$ (i.e., case 2 above), ΔS_{tot}^{min} arises entirely from the chemical reaction and is proportional to $N(\Delta t/N)^2$, despite the fact that the same reaction makes no contribution to ΔG_{tot}^{min} to order $N(\Delta t/N)^2$, as noted above. This circumstance occurs because with increasing T, the chemical reaction changes the equilibrium populations f_A° and f_B°, and thereby also the effective force constant in ΔG_{tot}^{min}. In fact, the chemical reaction contributes the same $N(\Delta t/N)^2$ term to both $T\Delta S_{tot}^{min}$ and ΔH_{tot}^{min}, so that term subtracts out of ΔG_{tot}^{min}. In this limit, ΔH_{tot}^{min} also contains another $N(\Delta t/N)^2$ term that arises from spring displacements at "frozen" chemical equilibrium, and that term is precisely ΔG_{tot}^{min}. Thus, in this limit, the shift in the chemical equilibrium makes no significant contribution to the twisting free energy, which is the same as for spring displacements at "frozen" chemical equilibrium, but it does contribute directly to the variation of the effective force constant with T, to ΔS_{tot}^{min}, and to ΔH_{tot}^{min}.

When the chemical reaction is shifted too far toward the lowest free energy state (say A), f_B° will be very small, and that will cause both $|d\langle\alpha\rangle/dT|$ and $|\Delta S_{tot}^{min}|$ to be very small, as can be seen from Eq. B16. This is the limit that might prevail in those DNAs that exhibit a negligible variation of $\langle\alpha\rangle$ with T. A more evenly balanced equilibrium with $f_A^\circ \approx f_B^\circ$ would admit a larger $|d\langle\alpha\rangle/dT|$ and $|\Delta S_{tot}^{min}|$. This is the circumstance that might prevail in the present 1876-bp DNA and other DNAs mentioned herein. Of course, such an explanation would require the equilibrium constant K for the chemical equilibrium between secondary structure states to vary strongly with sequence in at least some cases. Direct evidence for a long-range change in the secondary structure equilibrium that is induced by a particular change in sequence has been reported (Kim et al., 1993), as has evidence for a sequence-specific structural transition induced by increasing temperature (Chan et al., 1990).

Readers are cautioned that the simple noncooperative two-state model analyzed in Appendix B is surely a considerable oversimplification of the real system. Moreover, any change in secondary structure would most probably be accompanied by a change not only in intrinsic twist and twisting force constant, but also in the bending force constant and extent of intrinsic (permanent) bends. Nevertheless, the present model may provide useful insights into the possible molecular origins of the observed decline in $\langle\alpha\rangle$ with increasing T in the case of the present DNA and others recently studied in this laboratory (Delrow, 1996).

APPENDIX A: ENUMERATION AND CRITIQUE OF THE ASSUMPTIONS EMPLOYED TO EVALUATE SUPERCOILING FREE ENERGY, ENTHALPY, AND ENTROPY BY THE METHOD OF BAUER AND BENHAM

This new method either explicitly or implicitly invokes the following assumptions.

1. The molecular extensions and other deformations experienced during gel electrophoretic migration are implicitly assumed not to affect the supercoiling free energies and melting behavior.

2. The tertiary structure and gel mobility of a locally denatured topoisomer, which has a total linking difference Δl and a residual linking difference (Δl_r) associated with its nondenatured (i.e., duplex) regions, are assumed to be identical to the tertiary structure and gel mobility of a particular undenatured topoisomer, whose (lower) total linking difference exactly matches the Δl_r of the former molecule. This assumption is required to assess Δl_r by a comparison of the gel mobilities of denatured and undenatured species. However, if the flexural rigidity of the denatured regions is substantially less than that of normal duplex, as is almost certainly the case, then bending strain will accumulate preferentially in those regions. Although the effects of such flexurally soft regions on the tertiary structures and energetics of supercoiled DNAs have not yet been simulated, simulations of supercoiled DNAs containing permanent bends indicate clearly that such bends can cause extensive rearrangements of tertiary structure and that the intrinsically curved regions are found preferentially at the apices of superhelix branches (Kremer et al., 1993; Klenin et al., 1995; Diekmann and Langowski, 1995). Consequently, it seems rather unlikely that the tertiary structure and gel mobility of a topoisomer with a given Δl_r and one or more flexurally soft denatured regions will precisely match the tertiary structure and gel mobility of a completely undenatured topoisomer, whose Δl matches the Δl_r of the former.

3. It is assumed that any changes in the supercoiling enthalpy, entropy, and free energy of the undenatured regions due to the introduction of one or more flexurally soft zones in the denatured regions are entirely negligible. As noted above, there are reasons to suspect that this assumption may not be entirely correct.

4. It is assumed that every denatured region deforms torsionally, as if it were a uniform elastic filament with an effective torsion constant (α_d) between base pairs that is independent of either the length of the denatured region or the average torsional deformation (per base pair) from the untwisted equilibrium state. This assumed Hookean behavior was justified in terms of a Taylor series of the torsional free energy about the untwisted state. For a denatured region of sufficiently great size and sufficiently small torsional strain, the torsional free energy must be primarily entropic and stem from writhing of the single strands about each other, because they can individually undergo unrestricted twisting and are thus unable to store net twisting strain by themselves. However, in the experiments of Bauer and Benham (1993), the estimated torsional strain of the undenatured regions actually lies far outside this small deformation regime, as described below. The estimated torsion constant for the undenatured regions, namely $\alpha \simeq 1.08 \times 10^{-13}$ dyne cm at 310 K, is ~50 times smaller than that typical of normal duplex (Schurr et al., 1992); consequently the denatured regions will accumulate 50 times as much torsional strain as a duplex region of identical length (in base pairs) to maintain torque balance. In undenatured supercoiled DNAs, approximately one-third of Δl is partitioned into twist (Vologodskii and Cozzarelli, 1994). Hence, if $\Delta l = -15$ turns, then the net twisting strain is -5 turns molecule, or about -1.2×10^{-2} turns/10.4 bp. Under local denaturation conditions, where $\Delta l_r = -11$ turns for that same DNA, the twisting strain is assumed to decrease by the factor 11/15 in the duplex regions, to yield -0.9×10^{-2} turn/10.4 bp. However, in the denatured regions(s) this would be 50-fold larger, namely -0.45 turn/10.4 bp. This is almost one-half the equilibrium twist of normal duplex, but in the negative direction. Under such highly twisted conditions the two strands are expected to be in rather close van der Waals, H-bonding, and electrostatic "contact," so the torsional free energy of the duplex regions should acquire a substantial enthalpic component, as is found experimentally. In such a case, the torsional rigidity of the denatured region cannot be independent of torsional strain from the small strain limit up to the values manifested in the experiments of Bauer and Benham (1993). This observation does not invalidate the assumption of Hooke's law behavior over a limited range of large torsional deformations, but suggests that the effective torsion constant is not that applicable to the separated strands in the small deformation limit, and that the work required to torsionally deform the denatured region from its relaxed open circular state to its highly twisted final state has not been reckoned accurately. If the actual torsion constant ($\alpha_d(\tau)$) of the denatured region depends upon the mean torsional strain per base pair, and becomes identical to the high-strain value characteristic of the experiments only when the torsional strain τ itself exceeds some characteristic value τ_c, then the torsional free energy of the denatured region can be written as

$$n(\alpha_d/2)\tau^2 + n\int_0^{\tau_c} d\tau(\alpha_d(\tau) - \alpha_d)\tau$$

The first term corresponds to that assumed by Benham (1992) and Bauer and Benham (1993). The second (correction) term is also proportional to the length n of the denatured region. Consequently, omitting this correction from the data analysis is equivalent to assuming a transition free energy per base pair for denaturation that is equal to the stated value minus this correction term.

5. In the method of Bauer and Benham (1993), the supercoiling free energy is assessed not by its competition with RT, as is the case in topoisomer distribution experiments, but by its competition with the free energy of denaturation. Consequently, any errors in the assumed enthalpy and entropy of melting will be manifested directly in the estimated supercoiling free energy, enthalpy, and entropy. The correction term in the torsional free energy of the denatured region, mentioned above, is one potential source of such error. The melting free energy of each kind of base pair is extrapolated from its T_{mj} (j = A · T or G · C) by using the calorimetrically measured "average" enthalpies for each kind of base pair (Breslauer et al., 1986), which are assumed to be independent of T. The T_{mj} values are not corrected for differences in ionic conditions between the original calorimetric and subsequent strand separation measurements, although T_m is known to vary strongly with ionic strength (Bloomfield et al., 1974). For computational convenience, no account is taken of the different nearest-neighbor interactions between the different base pairs, which also may introduce significant error. Finally, the thermodynamic values of Breslauer et al. (1986) do not satisfactorily predict the relative melting temperatures of dumbbell DNAs, which are 40-bp single-strand loops that self-wind to form 16-bp duplexes with 4-T loops at either end, and which contain a common peripheral sequence with a variable 4-bp region in the middle (Benight et al., 1995; A. S. Benight, personal communication). They also do not match the optimal parameter set to account for those data. Because melting of such a molecule to an open single-strand loop is a better model for local denaturation than melting to two completely separated strands, the inadequacy of the thermodynamic parameters of Breslauer et al. (1986) in that application is particular cause for concern.

Besides the uncertain validity of the assumptions discussed above, certain peculiarities in the best-fit parameters extracted from the data of Bauer and Benham (1993) also sound a caution. The melting initiation parameter (a) is found to be independent of T, even though it is expected to contain a substantial ring entropy contribution that should be proportional to T. Moreover, a remains almost constant over nearly an order of magnitude range of ionic strength, whereas the torsion elastic constant of the denatured region is 4.3-fold larger in 10 mM Tris (pH 7.0) than in 90 mM Tris-borate (pH 8.4) (Benham, 1992; Bauer and Benham, 1993). It is surprising that the ionic strength modulates the torsional rigidity so strongly and the melting initiation parameter so little for an open region as short as 50–60 bp. Until some of the more questionable assumptions are properly tested by simulations and/or experiments, the quantitative results of Bauer and Benham must be considered less reliable than the results of direct calorimetry or topoisomer distribution experiments.

APPENDIX B: THERMODYNAMIC ANALYSIS OF THE TWISTING OF A CHAIN OF TWO-STATE SUBUNITS

We consider a chain of N connected subunits, each of which can exist in either of two states, A or B. The reaction

$$A \rightleftharpoons B \qquad \text{(B1)}$$

has equilibrium constant $K = f^\circ_B/f^\circ_A$, where f°_A and f°_B are the unperturbed equilibrium fractions in states A and B, respectively. The standard state free energy, enthalpy, and entropy changes per molecule for the unperturbed reaction (B1) are denoted by ΔG°, ΔH°, and ΔS°, respectively. Each subunit is imagined to consist of two separate rigid hemispheres that are attached to each other, not at their equators but at their poles by a Hookean torsion spring. When such subunits are connected end to end, they attach to their neighbors in the mutual equatorial planes, and there results a chain of rigid spheres separated by torsion springs, which terminates with a hemisphere at either end. The torsion spring of an A-subunit has an unperturbed twist ϕ°_A and a spring constant g_A, whereas that of a B-subunit has an unperturbed twist ϕ°_B and a spring constant g_B. The unperturbed twist of the chain of subunits is $t^\circ = N(f^\circ_A\phi^\circ_A + f^\circ_B\phi^\circ_B)$. When an overall twist (t) is imposed on the chain of subunits, the system is perturbed, so that the new fractions are $f_A = f^\circ_A + \delta f_A$, $f_B = f^\circ_B + \delta f_B$, and the new twists are $\phi_A = \phi^\circ_A + \delta\phi_A$, and $\phi_B = \phi^\circ_B = \delta\phi_B$. The total twist of the perturbed molecule is related to the local spring twists by $t = N(f_A\phi_A + f_B\phi_B)$.

At mechanical equilibrium (which also corresponds to the minimum of the free energy), the net torque on every sphere must vanish, which requires that $g_A\delta\phi_A = g_B\delta\phi_B$. When this vanishing torque condition is employed to eliminate $\delta\phi_A$, the total displacement of the twist (Δt) of the chain from its unperturbed value is given on a per-subunit basis by

$$\frac{\Delta t}{N} = \frac{t - t^\circ}{N} = (f^\circ_A(g_B/g_A) + f^\circ_B)\delta\phi_B + (\phi^\circ_B - \phi^\circ_A)\delta f_B + (1 - (g_B/g_A))\delta f_B\delta\phi_B \tag{B2}$$

The conservation condition $f_A + f_B = 1$ implies that $df_A = -\delta f_B$, which was used to eliminate δf_A from Eq. B2. If δf_B moles of reaction (B1) take place from the unperturbed equilibrium position, then the free energy change per subunit due to the reaction alone is

$$\frac{\Delta G_R}{N} = \delta f_B\left\{\Delta G^\circ + k_BT\ln\left(\frac{f^\circ_B + \delta f_B}{f^\circ_A + \delta f_A}\right)\right\} \tag{B3}$$

The total free energy difference per subunit between the twisted and untwisted chains is simply the sum of $\Delta G_R/N$ and the contributions from twisting the individual springs. After some algebra using relations cited above, there results

$$\frac{\Delta G_{tot}}{N} = \delta f_B k_BT\ln\left(\frac{f^\circ_B + \delta f_B}{f^\circ_B - K\delta f_B}\right) + (f^\circ_B + \delta f_B)\frac{g_B}{2}\delta\phi_B^2 + (f^\circ_A - \delta f_B)\frac{g_B}{2}(g_B/g_A)\delta\phi_B^2 \tag{B4}$$

The position of the perturbed equilibrium is found by minimizing $\Delta G^{tot}/N$ subject to the constraint of fixed $\Delta t/N$. We are concerned here with the Hooke's law regime wherein the total displacement per subunit, $\Delta t/N$, is small and $\Delta G^{tot}/N$ varies quadratically with $\Delta t/N$. Equation B2 is solved exactly to yield

$$\delta f_B = \frac{(\Delta t/N) - f^\circ_B((1/K)(g_B/g_A) + 1)\delta\phi_B}{\phi^\circ_B - \phi^\circ_A + (1 - (g_B/g_A))\delta\phi_B} \tag{B5}$$

In the limit of very small $\Delta t/N$, both δf_B and $\delta\phi_B$ are also very small, and the second term in the denominator can be neglected, except in the limit when $\phi^\circ_B - \phi^\circ_A \cong 0$ is also extremely small. That case ($\phi^\circ_B - \phi^\circ_A = 0$) will be treated separately. The linearized form of Eq. B5 (without the second term in the denominator) is inserted into Eq. B4. After expansion and segregation of all terms in Eq. B4 according to the order (power) of the small quantities, $\delta\phi_B$ and $\Delta t/N$, only the lowest (second-order) terms are retained. The validity of this expansion requires $|\delta f_B| \ll f^\circ_A, f^\circ_B$. Then Eq. B4 is minimized with respect to $\delta\phi_B$, while simultaneously holding Δt fixed and satisfying the vanishing torque condition ($\delta\phi_A = (g_B/g_A)\,\delta\phi_B$), to obtain (after some tedious algebra)

$$\delta\phi_B^{min} = \chi\Delta t/N \tag{B6}$$

where

$$\chi = \left[f^\circ_B\left(\frac{1}{K}\frac{g_B}{g_A} + 1\right) + \frac{f^\circ_B g_B(\phi^\circ_B - \phi^\circ_A)^2}{2k_BT(1 + K)}\right]^{-1} \tag{B7}$$

The corresponding minimum free energy difference between the twisted and untwisted chains is

$$\Delta G^{min}_{tot}/N = (g_B\chi/2)(\Delta t/N)^2 \tag{B8}$$

Thus, for sufficiently small total twists, $\delta\phi_B^{min}$ is proportional to $\Delta t/N$ and ΔG^{min}_{tot} varies quadratically with $(\Delta t/N)$, as expected.

To gain some further insight, we consider the following two limits.

1. If $g_B = g_A$, so there is no difference in spring constants between the A and B states, and at the same time $\phi^\circ_B - \phi^\circ_A \neq 0$ and the springs are very stiff, so that $(g_B/2)(\phi^\circ_B - \phi^\circ_A)^2 \gg k_BT$, and in addition $K \gtrsim 1$, then the second term in square brackets in Eq. B7 dominates. In this limit, $\chi \ll 1$ and $\delta\phi_B^{min} \ll \Delta t/N$ according to Eqs. B6 and B7, and

$$\delta f_B^{min} \cong (\Delta t/N)/(\phi^\circ_B - \phi^\circ_A) \tag{B9}$$

according to Eq. B5. The requirement, $\delta f_B^{min} \ll (f^\circ_A, f^\circ_B) < 1.0$, also implies that $\Delta t/N \ll \phi^\circ_B - \phi^\circ_A$. In this limit, the individual springs of the A and B states are so stiff that they are practically not displaced at all from their equilibrium positions, but instead the overall twist, Δt, is accommodated by shifting the chemical reaction so that the change, δf_B^{min}, is proportional to $\Delta t/N$. Also in this limit,

$$\Delta G^{min}_{tot}/N \cong \frac{2k_BT(1 + K)1}{2f^\circ_B(\phi^\circ_A - \phi^\circ_B)}\left(\frac{\Delta t}{N}\right)^2 \tag{B10}$$

$$\cong \frac{2k_BT(1 + K)}{2f^\circ_B}(\delta f_B^{min})^2 \tag{B11}$$

The free energy change in this case arises entirely from the shift in equilibrium position of the chemical reaction, and the effective force constant for $(\delta f_B^{min})^2$, namely $2k_BT(1 + K)/f^\circ_B$, is just k_BT times the inverse of the variance ($\langle(\delta f^2_B)\rangle$) of δf_B for the free unconstrained system, as expected from fluctuation theory (not shown). The work required to twist the chain in this limit is invested entirely in displacing the chemical equilibrium.

2. If $(\phi^\circ_B - \phi^\circ_A)$ is sufficiently small, or g_B is sufficiently small, or $(1/K)(g_B/g_A)$ is sufficiently large, then the first term in square brackets in Eq. B7 dominates. In this limit, Eq. B7 becomes

$$\Delta G^{min}_{tot}/N = (1/2)[f^\circ_A/g_A + f^\circ_B/g_B]^{-1}(\Delta t/N)^2 \tag{B12}$$

so the effective "force" constant for $\Delta t/N$ is simply the inverse of the weighted sum of inverse spring constants. This is precisely the same result that is obtained for a chain consisting of the same two types of springs, but in which the chemical reaction is "frozen" at its equilibrium position (Wilcoxon and Schurr, 1983). In this limit the chemical reaction makes no contribution to ΔG^{min}_{tot}, although it does contribute to ΔH^{min}_{tot} and ΔS^{min}_{tot}, as will be shown. In this limit the spring displacement,

$$\delta\phi_B^{min} = g_B^{-1}[f^\circ_B/g_B + f^\circ_A/g_A]^{-1}(\Delta t/N) \tag{B13}$$

is still proportional to $\Delta t/N$, but the shift (δf_B) of the chemical equilibrium vanishes to first order in $\Delta t/N$, because the numerator in Eq. B5 vanishes when $\delta\phi_B$ takes the value given in Eq. B13. The value of δf_B^{min} can be found in the following way. Equation B5 is solved for $\delta\phi_B$ (instead of δf_B),

$$\delta\phi_B = \frac{\Delta t/N - (\phi^\circ_B - \phi^\circ_A)\delta f_B}{f^\circ_B((1/K)(g_B/g_A) + 1) + (1 - (g_B/g_A))\delta f_B} \tag{B14}$$

This $\delta\phi_B$ and $\delta\phi_A = (g_B/g_A)\delta\phi_B$ are inserted into Eq. B4, which now contains only δf_B and $\Delta t/N$. That equation is minimized with respect to δf_B at constant $\Delta t/N$. Although the general solution is too complicated to present here, it simplifies in the limit $\phi_B^\circ - \phi_A^\circ = 0$ to give, in lowest (second) order,

$$\delta f_B^{\min} = (-1/2)\left(\frac{(g_B - g_A)}{g_A g_B[f_A^\circ/g_A + f_B^\circ/g_B]^2}\right)\left(\frac{f_B^\circ}{2k_BT(1+K)}\right)\left(\frac{\Delta t}{N}\right)^2 \tag{B15}$$

Thus, when $\phi_B^\circ - \phi_A^\circ = 0$, $\delta f_B^{\min}$ varies quadratically with $\Delta t/N$ to lowest nonvanishing order. Because the contribution of the chemical reaction, ΔG_R, varies quadratically with δf_B to lowest order in δf_B, in the present limit Eq. B15 implies that ΔG_R varies as $(\Delta t/N)^4$ to lowest order in $\Delta t/N$). Thus, in the present limit, ΔG_R simply does not contribute to $\Delta G_{tot}^{\min}$ to order $(\Delta t/N)^2$, and that is why the effective "force" constant in Eq. B12 is the same as for a "frozen" chemical equilibrium.

Although in this limit ($\phi_B^\circ - \phi_A^\circ = 0$) the chemical reaction makes no contribution to $\Delta G_{tot}^{\min}$ to order $(\Delta t/N)^2$, it does contribute an identical term of order $(\Delta t/N)^2$ to both $T\Delta S_{tot}^{\min}$ and $\Delta H_{tot}^{\min}$, which then subtracts out of $\Delta G_{tot}^{\min} = \Delta H_{tot}^{\min} - T\Delta S_{tot}^{\min}$. By using $f_B^\circ = K/(K+1)$, $f_A^\circ = 1/(K+1)$, $K = \exp[-(\Delta H^\circ - T\Delta S^\circ)/k_BT]$, and $\partial K/\partial T = (\Delta H^\circ/k_BT^2)K$, Eq. B12 can be directly differentiated with respect to T to obtain

$$\begin{aligned} T(\Delta S_{tot}^{\min}/N) &= -\partial(\Delta F_{tot}^{\min}/N)/\partial T \\ &= -\left(\frac{\Delta H^\circ}{k_BT}\right)f_B^\circ f_A^\circ\left(\frac{g_B - g_A}{2g_Bg_A[f_A^\circ/g_A + f_B^\circ/g_B]^2}\right)\left(\frac{\Delta t}{N}\right)^2 \end{aligned} \tag{B16}$$

provided the spring constants g_A and g_B do not change with T. In the present limit ($\phi_B^\circ - \phi_A^\circ = 0$), the entropy change of the twisting process is proportional to the standard enthalpy change, ΔH°, of the chemical reaction, and therefore arises entirely from that chemical reaction. Hence the chemical reaction contributes to $\Delta S_{tot}^{\min}$ to order $(\Delta t/N)^2$, although it does not contribute to $\Delta G_{tot}^{\min}$ to that same order. The enthalpy change of the twisting process is given by

$$\Delta H_{tot}^{\min}/N = \Delta G_{tot}^{\min}/N + T(\Delta S_{tot}^{\min}/N) \tag{B17}$$

and is readily evaluated from Eqs. B12 and B16. Hence in the present limit, wherein $\phi_B^\circ - \phi_A^\circ = 0$ and g_A and g_B are independent of T, $\Delta H_{tot}^{\min}$ consists of two contributions, one from spring displacement at constant ("frozen") chemical equilibrium and another from displacement of the chemical equilibrium, both of which are proportional to $(\Delta t/N)^2$.

In both the present case ($\phi_B^\circ - \phi_A^\circ = 0$) and in the more general case of Eq. B8, whenever the spring constants g_A and g_B and unperturbed twists ϕ_A° and ϕ_B° are independent of T, $\Delta S_{tot}^{\min}$ always contains the factor $\partial K/\partial T = (\Delta H^\circ/k_BT^2)K$ and hence is always proportional to ΔH° and therefore arises entirely from the chemical reaction. In the limit for which Eq. B16 applies, and when $g_B < g_A$, one finds that $\Delta S_{tot}^{\min}$ is positive, corresponding to a decreasing $\Delta G_{tot}^{\min}$ with increasing T, when ΔH° is positive. Because $\Delta S_{tot}^{\min}$ is proportional to ΔH°, but not ΔS°, one might inquire as to the fundamental origins of this entropy increase. In fact, the entropy change resides in the relative changes in the fractions, $\delta f_A/f_A^\circ$ and $\delta f_B/f_B^\circ$, of each kind of state. The entropic nature of these contributions is readily apparent from the $k_BT\ \ln[(f_B^\circ + \delta f_B)/(f_A^\circ + \delta f_A)]$ term in Eq. 3, from which those contributions originate. The ΔH° governs whether and how rapidly these fractions change in favor of the B state with increasing T.

The work was supported in part by grant GM32681 from the National Institutes of Health and grant MCB9317042 from the National Science Foundation.

REFERENCES

Allison, S. A., and J. M. Schurr. 1979. Torsion dynamics and depolarization of fluorescence of linear macromolecules. I. Theory and application to DNA. *Chem. Phys.* 41:35–59.

Barkley, M. D., and B. H. Zimm. 1979. Theory of twisting and bending of chain macromolecules; analysis of the fluorescence polarization anisotropy. *J. Chem. Phys.* 70:2991–3007.

Bauer, W. R., and C. J. Benham. 1993. The free energy, enthalpy, and entropy of native and of partially denatured closed circular DNA. *J. Mol. Biol.* 234:1184–1196.

Bauer, W. R., and R. Gallo. 1989. Physical and topological properties of closed circular DNA. *In* Chromosomes: Eukaryotic, Prokaryotic, and Viral, Vol. I. K. W. Adolph, editor. CRC Press, Boca Raton, FL. 87–126.

Benham, C. J. 1992. Energetics of the strand separation transition in superhelical DNA. *J. Mol. Biol.* 225:835–847.

Benight, A. S., F. J. Gallo, T. M. Paner, K. D. Bishop, B. D. Faldasz, and M. U. Lane. 1995. Sequence context and DNA reactivity: application to sequence-specific cleavage of DNA. *Adv. Biophys. Chem.* 5:1–55.

Bloomfield, V. A., D. M. Crothers, and I. Tinoco, Jr. 1974. Physical Chemistry of Nucleic Acids. Harper and Row, New York. 332–334.

Breslauer, K., R. Frank, H. Bloecker, and L. Marky. 1986. Predicting DNA stability from the base-pair sequence. *Proc. Natl. Acad. Sci. USA.* 83:3746–3750.

Chan, S. S., R. H. Austin, I. Mukerji, and T. G. Spiro. 1997. Temperature-dependent ultraviolet resonance Raman spectroscopy of the premelting state of dA·dT DNA. *Biophys. J.* 72:1512–1520.

Chan, S. S., K. J. Breslauer, R. H. Austin, and M. E. Hogan. 1993. Thermodynamics of premelting conformational changes of phased $(dA)_5$ tracts. *Biochemistry.* 32:11776–11784.

Chan, S. S., K. J. Breslauer, M. E. Hogan, D. J. Kesler, R. H. Austin, J. Ojemann, J. M. Passner, and N. C. Wiles. 1990. Physical studies of structural equilibria within periodic poly dA–poly dT sequences. *Biochemistry.* 29:6161–6171.

Clendenning, J. B., A. N. Naimushin, B. S. Fujimoto, D. W. Stewart, and J. M. Schurr. 1994. Effect of ethidium binding and superhelix density on the supercoiling free energy and torsion and bending constants of p30δ DNA. *Biophys. Chem.* 52:191–218.

Clendenning, J. B., and J. M. Schurr. 1994a. A model for the binding of *E. coli* single-strand binding protein to supercoiled DNA. *Biophys. Chem.* 52:227–249.

Clendenning, J. B., and J. M. Schurr. 1994b. Circularization of small DNAs in the presence of ethidium: a theoretical analysis. *Biopolymers.* 34:849–868.

Delrow, J. J. 1996. Evidence of alternative secondary structure states in DNA. Ph.D. thesis. University of Washington, Seattle, WA.

Delrow, J. J., J. A. Gebe, and J. M. Schurr. 1997. Comparison of hard-cylinder and screened Coulomb interactions in the modelling of supercoiled DNAs. *Biopolymers.* (in press).

Depew, R. E., and J. C. Wang. 1975. Conformational fluctuations of the DNA helix. *Proc. Natl. Acad. Sci. USA.* 72:4275–4279.

Diekmann, S., and J. Langowski. 1995. Supercoiling couples DNA curvature to the overall shape and the internal motion of the DNA molecule in solution. *Theochemistry.* 336:227–334.

Duguet, M. 1993. The helical repeat of DNA at high temperature. *Nucleic Acids Res.* 21:463–468.

Frank-Kamenetskii, M. D., A. V. Lukashin, V. V. Anshelevich, and A. V. Vologodskii. 1985. Torsional and bending rigidity of the double helix from data on small DNA rings. *J. Biomol. Struct. Dyn.* 2:1005–1012.

Frank-Kamenetskii, M. D., and A. V. Vologodskii. 1981. Topological aspects of the physics of polymers: the theory and its biophysical applications. *Sov. Phys. Usp.* 24:679–696.

Fujimoto, B. S., and J. M. Schurr. 1990. Dependence of the torsional rigidity of DNA on base-composition. *Nature.* 344:175–178.

Gebe, J. A., S. A. Allison, J. B. Clendenning, and J. M. Schurr. 1995. Monte Carlo simulations of supercoiling free energies for unknotted and trefoil knotted DNAs. *Biophys. J.* 68:619–633.

Gebe, J. A., J. J. Delrow, P. J. Heath, D. W. Stewart, and J. M. Schurr. 1996. Effects of Na^+ and Mg^{2+} ions on the structures of supercoiled DNAs. Comparison of simulations with experiments. *J. Mol. Biol.* 262:105–128.

Gellert, M. 1981. DNA topisomerases. *Annu. Rev. Biochem.* 50:879–910.

Heath, P. J., J. B. Clendenning, B. S. Fujimoto, and J. M. Schurr. 1996. Effect of bending strain on the torsion elastic constant of DNA. *J. Mol. Biol.* 260:718–730.

Herrera, J. E., and J. B. Chaires. 1989. A premelting conformational change in poly dA-poly dT coupled to daunomycin binding. *Biochemistry.* 26:1993–2000.

Horowitz, D. S., and J. C. Wang. 1984. Torsional rigidity of DNA and length dependence of the free energy of supercoiling. *J. Mol. Biol.* 173:75–91.

Hustedt, E. J., A. Spaltenstein, J. E. Kirchner, C. Mailer, P. B. Hopkins, and B. H. Robinson. 1993. Motions of short DNA duplexes: an analysis of DNA dynamics using an epr-active probe. *Biochemistry.* 32: 1774–1787.

Kim, U. S., B. S. Fujimoto, C. E. Furlong, J. A. Sundstrom, R. Humbert, D. C. Teller, and J. M. Schurr. 1993. Dynamics and structures of DNA: long-range effects of a 16 base-pair $(CG)_8$ sequence on secondary structure. *Biopolymers.* 33:1725–1745.

Klenin, K. V., M. D. Frank-Kamenetskii, and J. Langowski. 1995. Modulation of intramolecular interactions in superhelical DNA by curved sequences. A Monte Carlo study. *Biophys. J.* 68:81–88.

Klenin, K. V., A. V. Vologodskii, V. V. Anshelevich, A. M. Dykhne, and M. D. Frank-Kamenetskii. 1991. Computer simulation of DNA supercoiling. *J. Mol. Biol.* 217:413–419.

Kowalski, D., D. A. Natale, and M. J. Eddy. 1988. Stable DNA unwinding, not "breathing," accounts for single-strand-specific nuclease hypersensitivity of specific A + T-rich sequences. *Proc. Natl. Acad. Sci. USA.* 85:9464–9468.

Kremer, W., K. Klenin, S. Diekmann, and J. Langowski. 1993. DNA curvature influences the internal motion of superhelical DNA. *EMBO J.* 12:4407–4412.

Langowski, J., A. S. Benight, B. S. Fujimoto, and J. M. Schurr. 1985. Change of conformation and internal dynamics of supercoiled DNA upon binding of *E. coli* single-strand binding protein. *Biochemistry.* 24:4022–4028.

Naimushin, A. N., J. B. Clendenning, U. S. Kim, L. Song, B. S. Fujimoto, D. W. Stewart, and J. M. Schurr. 1994. Effect of ethidium binding and superhelix density on the apparent supercoiling free energy and torsion constants of pBR322 DNA. *Biophys. Chem.* 52:219–226.

Parekh, B., and G. W. Hatfield. 1996. Transcriptional activation by protein-induced DNA bending: evidence for a DNA structural transmission model. *Proc. Natl. Acad. Sci. USA.* 93:1173–1177.

Pulleyblank, D. E., M. Shure, D. Tang, J. Vinograd, and H. P. Vosberg. 1975. Action of nicking-closing enzyme on supercoiled and nonsupercoiled closed circular DNA: formation of a Boltzmann distribution of topological isomers. *Proc. Natl. Acad. Sci. USA.* 72:4280–4284.

Reese, A. 1996. Analysis of cw-epr linewidths and the internal dynamics of DNA. Ph.D. thesis. University of Washington, Seattle, WA.

Rippe, K., P. H. von Hippel, and J. Langowski. 1995. Action at a distance: DNA looping and initiation of transcription. *Trends Biochem. Sci.* 20: 500–506.

Robinson, B. H., L. S. Lerman, A. Beth, H. L. Frisch, L. R. Dalton, and C. Auer. 1980. Analysis of double-helix motions with spin-labeled probes: binding geometry and the limit of torsional elasticity. *J. Mol. Biol.* 139:19–44.

Schurr, J. M., and B. S. Fujimoto. 1988. The amplitude of local angular motions of intercalated dyes and bases in DNA. *Biopolymers.* 27: 1543–1569.

Schurr, J. M., B. S. Fujimoto, P. Wu, and L. Song. 1992. Fluorescence studies of nucleic acids: dynamics, rigidities and structures. *In* Topics in Fluorescence Spectroscopy, Vol. 3, Biochemical Applications. J. R. Lakowicz, editor. Plenum Press, New York. 137–229.

Seidl, A., and H.-J. Hinz. 1984. The free energy of DNA supercoiling is enthalpy determined. *Proc. Natl. Acad. Sci. USA.* 81:1312–1316.

Selvin, P. R., D. N. Cook, N. G. Pon, W. R. Bauer, M. P. Klein, and J. E. Hearst. 1991. Torsional rigidity of positively and negatively supercoiled DNA. *Science.* 255:28–31.

Shibata, J. H., J. Wilcoxon, J. M. Schurr, and V. Knauf. 1984. Structures and dynamics of a supercoiled DNA. *Biochemistry.* 23:1188–1194.

Shimada, J., and H. Yamakawa. 1985. Statistical mechanics of DNA topoisomers. The helical wormlike chain. *J. Mol. Biol.* 184:319–329.

Shore, D., and R. L. Baldwin. 1983. Energetics of DNA twisting II. Topoisomer analysis. *J. Mol. Biol.* 170:983–1007.

Song, L., B. S. Fujimoto, P. Wu, J. C. Thomas, J. H. Shibata, and J. M. Schurr. 1990. Evidence for allosteric transitions in secondary structure induced by superhelical stress. *J. Mol. Biol.* 214:307–326.

Stigter, D. 1977. Interactions of highly charged colloidal cylinders with applications to double-stranded DNA. *Biopolymers.* 16:1435–1438.

Taylor, W. H., and P. J. Hagerman. 1990. Application of the method of T4 phage ligase-catalyzed ring-closure to the study of DNA structure. II. NaCl-dependence of DNA flexibility and helical repeat. *J. Mol. Biol.* 212:363–376.

Thomas, J. C., and J. M. Schurr. 1983. Fluorescence depolarization and temperature dependence of the torsion elastic constant of linear $\phi 29$ DNA. *Biochemistry.* 22:6194–6198.

Vologodskii, A. V., and N. R. Cozzarelli. 1994. Conformational and thermodynamic properties of supercoiled DNA. *Annu. Rev. Biophys. Biomol. Struct.* 23:609–643.

Wang, J. C. 1985. DNA topoisomerases. *Annu. Rev. Biochem.* 54: 665–697.

Wilcoxon, J. P., and J. M. Schurr. 1983. Temperature dependence of the dynamic light scattering of linear $\phi 29$ DNA: implications for spontaneous opening of the double-helix. *Biopolymers.* 22:2273–2321.

Wu, P.-G., B. S. Fujimoto, and J. M. Schurr. 1987. Time-resolved fluorescence polarization anisotropy of short restriction fragments: the friction factor for rotation of DNA about its symmetry axis. *Biopolymers.* 26:1463–1488.

Wu, P.-G., B. S. Fujimoto, L. Song, and J. M. Schurr. 1991. Effect of ethidium on the torsion constants of linear and supercoiled DNAs. *Biophys. Chem.* 41:217–236.

Wu, P.-G., and J. M. Schurr. 1989. Effects of chloroquine on the torsional dynamics and rigidities of linear and supercoiled DNAs at low ionic strength. *Biopolymers.* 28:1695–1703.

Wu, P.-G., L. Song, J. B. Clendenning, B. S. Fujimoto, A. S. Benight, and J. M. Schurr. 1988. Interaction of chloroquine with linear and supercoiled DNAs. Effect on the torsional dynamics, rigidity, and twist energy parameter. *Biochemistry.* 27:8128–8144.